Journal of the Mechanical Behavior of Biomedical Materials 80 (2018) 104–110

Contents lists available at ScienceDirect

Journal of the Mechanical Behavior of Biomedical Materials

journal homepage: www.elsevier.com/locate/jmbbm

Larger vertebral endplate concavities cause higher failure load and work at failure under high-rate impact loading of rabbit spinal explants

S. Dudli[a,b,d,*], W. Enns-Bray[b], Y. Pauchard[c], A. Römmeler[b], A.J. Fields[d], S.J. Ferguson[b], B. Helgason[b,e]

[a] University Hospital Zurich, Center of Experimental Rheumatology, Lengghalde 5, 8008 Zurich, Switzerland
[b] ETH Zurich, Institute for Biomechanics, Hönggerbergring 64, 8093 Zürich, Switzerland
[c] University of Calgary, McCaig Inst. for Bone and Joint Health, 2500 University Dr, Calgary, Canada
[d] University of California San Francisco, Department of Orthopaedic Surgery, 513 Parnassus Ave, 94143 San Francisco, United States
[e] School of Science and Engineering, Reykjavik University, Menntavegur 1, Reykjavík, Iceland

ARTICLE INFO

Keywords:
Endplate
Vertebra
Intervertebral disc
Fracture
Morphometry
High-rate

ABSTRACT

Vertebral fractures are among the most common of all osteoporosis related fracture types and its risk assessment is largely based on bone quality measures. Morphometric parameters are not yet considered, although endplate thickness and concavity shape were found to be important in fracture prediction in low-rate tests. We hypothesized that, under high-rate impact loading, the shape and size of the central endplate concavity are of key importance for fracture prediction. Therefore, we tested rabbit spinal segment explants in vitro under high-rate impact loading. With a combination of microCT to describe endplate morphometry, high-speed video imaging, and impact force measurement, endplate morphometry was correlated to the mechanical response. We found that endplate concavity shape and volume were important in describing the mechanical response: larger concavities caused higher failure load. We suggest a model for the fracture mechanism under high-rate impact loading, considering the morphometry of the endplates: wider and more voluminous concavities are protective whereas steeper slopes of the concavity edges and increasing bone volume fraction of the central endplate moiety are disadvantageous. Therefore, the shape and size of endplate morphometry are important in vertebral fracture prediction and should be considered included in vertebral fracture risk assessment.

1. Introduction

Vertebral compression fracture are among the most common of all osteoporosis-related fracture types (Riggs and Melton, 1986). Twenty-five percent of postmenopausal women in the US are affected by vertebral compression fractures, which increases their mortality rate by 15% (Old and Calvert, 2004). Clinical assessment of vertebral fracture risk utilizes DXA- or QCT-based measures of bone quantity in combination with gender, age, prior fracture history, and a number of lifestyle factors (Hulme et al., 2007; Krege et al., 2013). However, vertebral strength — and therefore, fracture risk — is also affected by vertebral geometry (Genant et al., 1993; Tatoń et al., 2014), trabecular microarchitecture (Hulme et al., 2007), cortical shell morphology (Fields et al., 2009; Roux et al., 2010, 2016), and disc degeneration (Adams et al., 1996). The thickness and shape of the endplate, which is the weakest link in the spine, may also be important (Jackman et al., 2016, 2014). For example, under slow compressive loading rates, thicker endplates with bigger concavities have higher maximal strains (Nekkanty et al., 2010) and yield stresses (Zhao et al., 2009). Larger concavities may decrease stress in the subchondral bone below the central endplate (Langrana et al., 2006) and therefore be protective against vertebral fractures and improve the diagnostic performance of fracture risk prediction tools. However, vertebral compression fractures in less than severe osteoporosis requires an impact trauma, e.g. falling from a chair or tripping (Old and Calvert, 2004). Yet the effects of endplate morphometry on strength and fracture mechanism have not been studied under high loading rates, which could influence fracture mechanism (Brown et al., 2008; Dudli et al., 2011; El-Rich et al., 2009; Tran et al., 1995; Wagnac et al., 2012) and alter the importance of endplate morphometry that has been observed at slow loading rates. Therefore, the aim of this sudy was to investigate the effects of endplate morphometric parameters on vertebral strength and fracture mechanism under high-rate impact loading. To do this, we combined an established model for generating high-rate impact loading on rabbit vertebra explants (Dudli et al., 2012) with high-resolution microCT analysis of endplate morphometry, high-speed video imaging, and

* Corresponding author at: University Hospital Zurich, Center of Experimental Rheumatology, Lengghalde 5, 8008 Zürich, Switzerland.
E-mail address: Stefan.Dudli@usz.ch (S. Dudli).

https://doi.org/10.1016/j.jmbbm.2018.01.019
Received 4 July 2017; Received in revised form 14 December 2017; Accepted 17 January 2018
1751-6161/ © 2018 Elsevier Ltd. All rights reserved.

impact force measurement. We hypothesized that the shape and size of endplate concavity affects vertebral fracture mechanism under high-rate impact loading.

2. Material and methods

An overview of the workflow is provided in Supplement 1.

2.1. Specimen acquisition and preparation

Spinal segments (disc/endplates + 1/3 vertebrae) were harvested from T10/T11-L5/6 (n = 16) from two skeletally sub-mature New Zealand White rabbits (female, 6 months old) with microsurgical technique. The two vertebral cross section surfaces were leveled, prepared parallel to each other, and perpendicular with respect to the cranial/caudal axis of the segment. The axis was established by visual inspection of the segments during the preparation procedure. If the cross-sectional surfaces is not prepared perpendicular to the caudal-cranial axis, herniations or lateral pincer fracture occur. This was analyzed by dissecting specimens after impact loading. This is important since these are the contact areas with the aluminum caps of the fracture and loading devices. Specimens were stored at −20 °C, wrapped with a gauze soaked in phosphate-buffered saline (PBS).

2.2. Micro-CT and morphometric parameters

Specimens were scanned with a µCT 100 (20 µm voxel size, 45 kVp, 200 µA, 204 ms integration time, SCANCO Medical, Brüttisellen, Switzerland) while being soaked in PBS. From µCT scans the following morphometric variables were calculated for the caudal ("CaXX"; caudal relative to the disc) and cranial endplates ("CrXX"): average endplate thickness (CaTh, CrTh), bone volume fraction (CaBV/TV, CrBV/TV), maximal width (CaW, CrW), maximal depth (CaD, CrD), maximal slope (CaS, CrS), and total volume (CaV, CrV) of the concavity (Fig. 1). Concavity width, depth, slope, and area were calculated for each sagittal image using custom ImageJ (v1.46R, Bethesda, MD, USA) and R (v3.02) scripts. For each image, first, the tangential line connecting both boarders of the concavity was calculated. The distance between the two points of contact (pc1, pc2) was the concavity width. Depth was calculated as the longest perpendicular distance from the tangential line to the concavity bottom (cb). Slopes were calculated as the angles pc1-pc2-cb and pc2-pc1-cb. The maximal values over all images for width, depth, and slope were considered as maximal width, depth and slope. For each image, the area between the tangential line and the endplate was calculated and multiplied with the voxel size to obtain a concavity volume slice. Summing up all concavity volume slices from all images resulted in the total concavity volume. Endplate thickness and BV/TV were calculated for the area of the central concavity (cylindric area at largest concavity depth with a diameter of maximal concavity width).

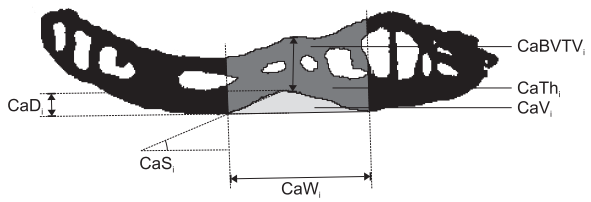

Fig. 1. Mid-sagittal reconstructed µCT image of a caudal (Ca) endplate with part of subchondral bone until growth plate. Depth (D_i), width (W_i), volume (V_i, light grey), and slope (S_i) of concavity were calculated for each sagittal slide. Integrated volume (V) and maximal D, W, and S and over all slides were used as endplate specific morphometric parameters. Endplate thickness (Th) and bone volume fraction (BVTV, dark grey) was calculated between the intervertebral disc and the growth plate for a central core defined by the concavity width. Endplate thickness was averaged for each slide and then over all slides.

Minimal disc height (H) was calculated from µCT by calculating the voronoi line between the two endplates on each sagittal image. The voronoi line is the line consisting of points which are equidistant to both endplates. From each image and then from all images, the minimal distance is calculated. Reconstructed 3D top-view onto endplates (point of view = intervertebral disc) without 3D-perspective were used to visualize endplates. The entire visible area was considered as endplate cross-sectional area. The average of the cranial and caudal cross-sectional area was used as endplate cross-sectional area (A).

2.3. High-rate impact loading and mechanical parameters

Specimens were glued using a fast-setting cyanoacrylate glue (UHU GmbH, Bühl, Switzerland) in parallel aluminum caps, which guarantee pure axial loading during compression. If necessary, the cross section surface was further leveled with microsurgical technique so that the entire cross section surface touched the aluminum cap and allowed even load distribution and axial loading. Fractures were induced by dropping a weight of 0.53 kg from a height of 19.5 cm, resulting in a target impact speed of 1.95 m/s and a nominal impact energy of 1 J. This energy was shown to introduce a reproducible endplate fracture (Dudli et al., 2011). Mechanical tests and computer simulations of high rate compressive loading in previous studies used velocities from 1 m/s to 6.3 m/s (Dooley et al., 2013; Ochia et al., 2003; Panjabi et al., 2000; Tran et al., 1995; Wagnac et al., 2012; Wilcox et al., 2003). Force during loading was measured with an impact load cell (Kistler 9321 A, 250 kHz, Sindelfingen, Germany) fixed under the specimen and events were recorded with a high-speed video camera (MotionPro Y8-S3, IDT (UK) Ltd, Herts, UK) at a 24 kHz sampling rate, Experimental mechanical data were maximal displacement (d), failure load (F), work at failure (E), displacement rate (e), compliance (C), and Boolean parameters (i.e. true, false) for which endplate fractured under impact loading (CaF, CrF). For the calculation of the work at failure, the average displacement rate and compliance, video data were analyzed using an in-house software programed in MATLAB (R2015b, The MathWorks Inc. (USA)). Displacement of the superior end-cap was tracked frame-by-frame, using semi-automated edge detection based on contrast between the illuminated aluminum endcap and the black background. MATLAB's cubic smoothing spline function was used to fit a curve to the load cell data. Failure load was defined as the first peak of the force measured by the load cell divided by the mean area of each specimen, and maximum displacement was defined as the displacement at maximum stress. Compliance was defined manually by measuring the slope of the linear region of the force-displacement curve (synchronized at the onset of impact) (Supplement 2). For specimens with non-linear behavior, the maximum tangential slope was used to define compliance. Work at failure was defined as the area under the force-displacement curve from the onset of impact up until maximum force, and was evaluated using MATLAB's trapezoidal numerical integration function.

2.4. Statistical model

For statistical calculations, the software R was used (R Core Team, v3.0.2, 2013, Vienna). All morphometric and mechanical variables were tested for normal distribution using Shapiro-Wilk test and for heteroscedasticity with the Breusch-Pagan test. Three different correlation analysis were done:

(i) Morphometric data from cranial and caudal endplates were compared with paired Wilcoxon tests, e.g. CaTh vs CrTh. Although most variables were normally distributed, conservative rank tests were used due to limited replicate numbers.
(ii) Correlations between morphometric and mechanical parameter were calculated using Spearman's correlation. P-values were adjusted for multiple testing using false discovery rate. The

Download English Version:

https://daneshyari.com/en/article/7207148

Download Persian Version:

https://daneshyari.com/article/7207148

Daneshyari.com